Genomics 92 (2008) 393–399

Contents lists available at ScienceDirect

Genomics

journal homepage: www.elsevier.com/locate/ygeno

Neuroendocrine and immune network re-modeling in chronic fatigue syndrome: An exploratory analysis

Jim Fuite [a], Suzanne D. Vernon [b], Gordon Broderick [a,*]

[a] Department of Medicine, Division of Pulmonary Faculty of Medicine and Dentistry, University of Alberta, 2E4.41 Walter Mackenzie Health Sciences Centre, 8440-112 Street, Edmonton, AB, Canada
[b] The Chronic Fatigue and Immune Dysfunction Syndromes (CFIDS) Association of America, Charlotte, NC, USA

ARTICLE INFO

Article history:
Received 16 February 2008
Accepted 17 August 2008
Available online 1 October 2008

Keywords:
Endocrine
Chronic fatigue
Co-expression
Networks
Graph theory
Centrality
Connectivity
Immune function
Signaling

ABSTRACT

This work investigates the significance of changes in association patterns linking indicators of neuroendocrine and immune activity in patients with chronic fatigue syndrome (CFS). Gene sets preferentially expressed in specific immune cell isolates were integrated with neuroendocrine data from a large population-based study. Co-expression patterns linking immune cell activity with hypothalamic–pituitary–adrenal (HPA), thyroidal (HPT) and gonadal (HPG) axis status were computed using mutual information criteria. Networks in control and CFS subjects were compared globally in terms of a weighted graph edit distance. Local re-modeling of node connectivity was quantified by node degree and eigenvector centrality measures. Results indicate statistically significant differences between CFS and control networks determined mainly by re-modeling around pituitary and thyroid nodes as well as an emergent immune sub-network. Findings align with known mechanisms of chronic inflammation and support possible immune-mediated loss of thyroid function in CFS exacerbated by blunted HPA axis responsiveness.

Introduction

Chronic fatigue syndrome (CFS) is a disorder linked to chronic immune activation [1] and dysregulation of the hypothalamic–pituitary–adrenal (HPA) axis [2,3]. Significant shifts in immune T, B and NK cell populations and effectiveness have been reported in CFS [4,5]. These upsets in immune demographics are accompanied by altered levels of inflammatory signaling via specific cytokine molecules [6]. The HPA axis is central in modulating this inflammatory response using feedback and feed forward control involving corticotropin-releasing hormone (CRH), adrenocorticotropic hormone (ACTH) and the synthesis of cortisol [2]. Cortisol induces a down-regulation of inflammation that is monitored by cytokine receptors located along the HPA axis [7], a mechanism that appears disrupted in typically hypocortisolic CFS patients [3]. We propose that this disruption results not only from the possible failure of individual neuro-immune components but also involves a spontaneous restructuring of this control network.

Markers of neuroendocrine and immune status tend to be highly variable and context-specific leading to inconsistent biomarker lists [8,9]. Such indicators describe an integrated system and their interdependency must be addressed formally. Accordingly, there is a growing interest in the network analysis of known pathways [10,11]. It is important to note however that these analyses do not attempt to identify changes in the patterns of association separating networks. Instead they focus solely on identifying associations between nodes that are differentially expressed across disease groups. This restriction can lead to the loss of important network features. In a novel exception, activation thresholds have been used to recover instances of validated molecular interactions from microarray data [12]. However such theory-driven approaches can only recover currently documented interactions and consequently remain limited in scope. Broader data-driven approaches such as multivariate factor analysis have been used to identify linear combinations of genes and proteins that correlate with disease state [13–15]. While these methods address aspects of combinatorial complexity and redundancy in biology, they are not used to describe changes in network structure. Knowledge of topological features in biological networks and their impact on function is needed if we are to understand complex illnesses [16].

Only recently has graph theory been formally applied to the comparative analysis of structure in biological networks [17]. Of particular relevance to this work are undirected graphs constructed by Emmert-Streib [18] to describe gene set co-expression in CFS. We extend this work in several important ways. First, we establish gene sets that represent the activity of specific immune cell types facilitating reconciliation with published cytometry findings. Second, we incorporate data describing hypothalamic–pituitary–adrenal (HPA), thyroidal

* Corresponding author. Fax: +1 780 407 6384.
E-mail address: gordon.broderick@ualberta.ca (G. Broderick).

0888-7543/$ – see front matter © 2008 Elsevier Inc. All rights reserved.
doi:10.1016/j.ygeno.2008.08.008

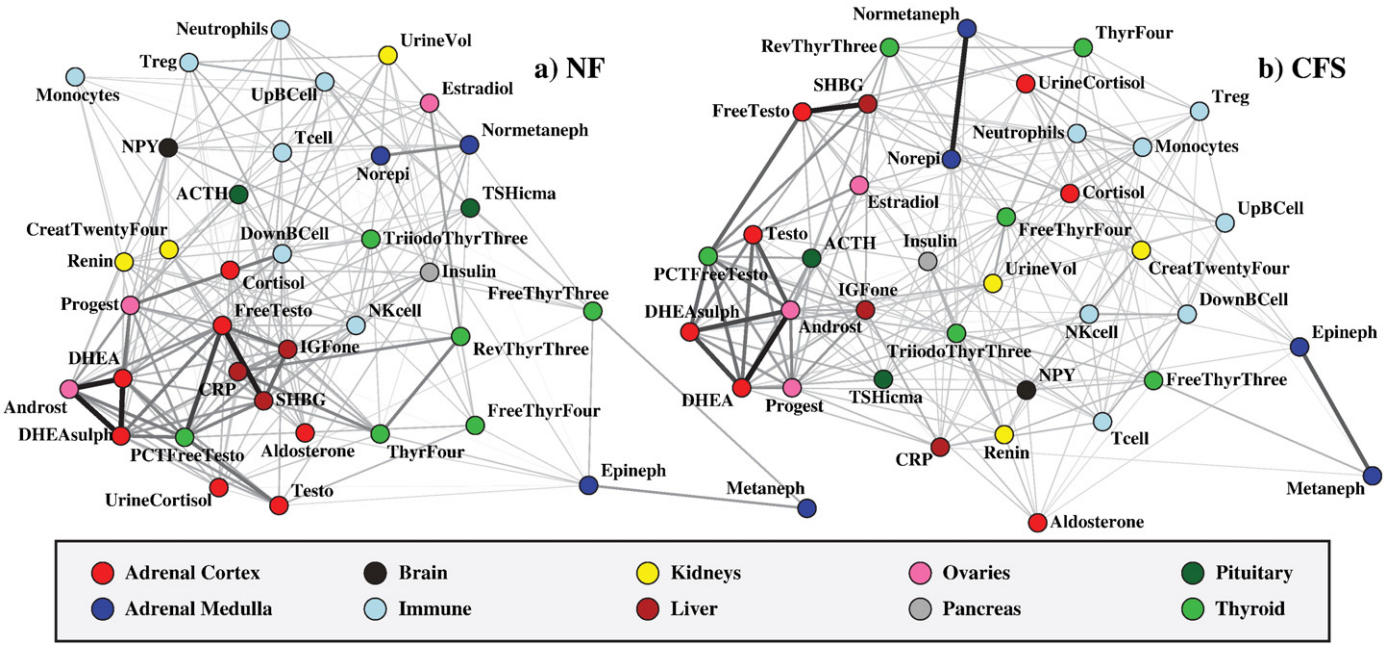

Fig. 1. CFS and NF networks are visibly different in topology. Spring-electrical embedding of mutual information networks mapping the interactions between 30 neuroendocrine measures and 7 immune cell gene sets constructed using within-group variation in 37 non-fatigued control subjects (a) and 39 CFS patients (b). All edge weights are significant at $p \leq 0.001$.

(HPT) and gonadal (HPG) axis status. Furthermore, mutual information (MI) rather than Pearson's correlation measure is used to capture nonlinear patterns of association [19]. Finally, we analyze edges weighted with their respective MI values instead of conventional present–absent assignments. To quantify differences in graph size and structure we use weighted graph edit distance and apply local measures of connectivity to identify key drivers of network re-modeling.

Results

Differential expression does not adequately describe CFS

The Wilcoxon rank sum test revealed that only 2 of 30 neuroendocrine functional indicators changed in median value ($p \leq 0.05$) in CFS versus non-fatigued controls (NF) (Supplementary Table S1). Circulating aldosterone was significantly higher in CFS versus NF. Thyroid function was also altered with significantly lower levels of unbound thyroxin (free T4) in CFS. Similarly of the 7 gene sets describing immune activation only the CD19+ B cell up-regulated set was differentially expressed at $p \leq 0.05$ (Supplementary Table S2). Expression of these normally up-regulated genes was found to be significantly lower in CFS. In summary, only 3 of 37 neuroendocrine and immune indicators were significantly altered ($p \leq 0.05$).

Global neuroendocrine and immune restructuring in CFS

Networks were built separately for CFS and NF using within-group variability to estimate pair-wise mutual information (MI) linking all 30 neuroendocrine nodes and nodes corresponding to the 7 immune gene sets (Fig. 1). Summary network statistics are shown in Table 1. Interestingly, network size or the total number of edges was essentially conserved between these two relatively well-connected networks. A total of 209 edges linked NF network nodes with a cumulated edge weight of 4.48 compared to 208 edges and a cumulated edge weight of 4.21 in CFS. Individual nodes carried between 2 and 16 edges with the average node having 11. Average node degree centrality (~0.228–0.242) and node eigenvector centrality (~0.182–0.180) were also similar in both CFS and NF.

While similar in overall connectivity, the networks in Fig. 1 remained visibly different in topology. Indeed the distribution of centrality among the nodes within each network was markedly different. The overall network centrality index increased in CFS, driven mainly by the neuroendocrine sub-network since the immune sub-network decreased in centrality (Table 1). CFS and NF networks were separated by a weighted edit distance of ~4.99 or ~4.72 when adjusted for graph size as a result of this restructuring (Figure S2). This corresponded to 120 standard deviations (0.04) above the expected distance between two networks constructed from randomly sampled NF subjects (~0.29) and 4 standard deviations (~0.06) above the expected separation between two multi-graphs (~1.38) conserving node degree. Local restructuring was described by changes in node

Table 1
Summary of mean and standard error ( ) values for network-wide descriptive metrics in NF and CFS

Network	Metric	NF	CFS
Overall network	Centrality index	0.40 (0.001)	0.46 (0.001)
	Total cumulated edge weight (size)	4.48 (0.009)	4.21 (0.014)
	Total number edges	209.60 (0.371)	208.10 (0.288)
	Node degree centrality	0.24 (0.018)	0.23 (0.013)
	Node eigenvector centrality	0.18 (0.024)	0.18 (0.024)
	Edges per node	11.33 (0.470)	11.25 (0.014)
Immune sub-network	Centrality index	0.64 (0.002)	0.31 (0.003)
	Total cumulated edge weight (size)	0.16 (0.000)	0.25 (0.001)
	Total number edges	9.00 (0.000)	15.00 (0.000)
	Node degree centrality	0.05 (0.009)	0.07 (0.004)
	Node eigenvector centrality	0.47 (0.107)	0.53 (0.028)
	Edges per node	2.57 (0.481)	4.29 (0.184)
Neuroendocrine sub-network	Centrality index	0.42 (0.001)	0.47 (0.001)
	Total cumulated edge weight (size)	3.32 (0.007)	3.27 (0.011)
	Total number edges	143.60 (0.275)	148.20 (0.224)
	Node degree centrality	0.22 (0.020)	0.22 (0.016)
	Node eigenvector centrality	0.20 (0.031)	0.20 (0.029)
	Edges per node	9.57 (0.482)	9.88 (0.421)

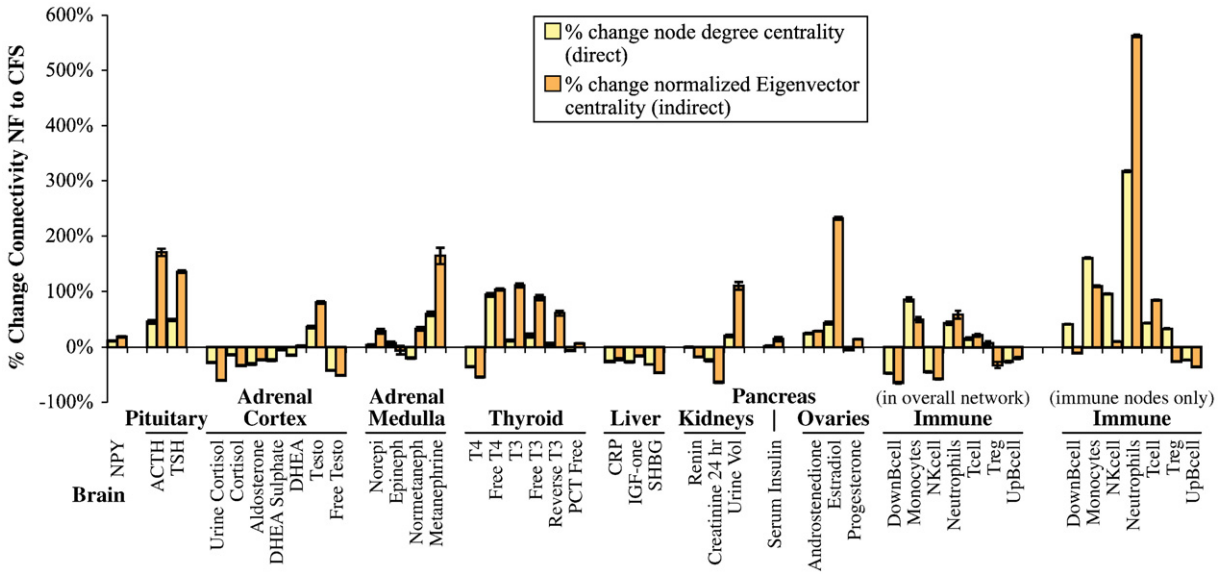

Fig. 2. Pituitary, thyroid, ovarian and immune functional nodes alter connectivity. Details of relative change in the total weight of edges connected at each node (node degree centrality) as well as edges acquired through first neighbors (normalized eigenvector centrality). Neuroendocrine nodes associated with pituitary and thyroid function are much better integrated with the greater network in CFS whereas adrenal cortex function is uniformly less integrated. Exceptionally metanephrine and estradiol nodes also increase connectivity. Monocyte and neutrophil immune functional nodes are more connected both within the immune sub-network and with nodes of the extended neuroendocrine network in CFS. In contrast NK cell and down-regulated B cell nodes dissociate from the larger network in favor of increased connectivity to other lymphocyte functional nodes.

degree centrality, a measure of direct connectivity, and eigenvector centrality, a measure of indirect connectivity. Results in Fig. 2 indicated that nodes associated with pituitary, thyroid and ovarian function generally increased their direct connectivity to the larger network in CFS and in doing so generally favored association with influential neighbors. For example, nodes for ACTH and thyroid stimulating hormone (TSH) increased their direct links by a factor of 1.5 while more than doubling their normalized eigenvector centrality. Free T4 as well as bound and free triiodothyronine (T3) nodes also doubled in eigenvector centrality in CFS while estradiol virtually tripled its indirect connectivity. In contrast, nodes associated with adrenal cortex, liver and kidney function were generally less integrated with the neuroendocrine network in CFS. Both cortisol nodes decreased their direct and indirect association with other nodes by half or more. In an exception to the general trend for thyroid function, bound T4 also decreased in connectivity in CFS.

ACTH activity was decoupled from B and T cell responses in CFS (Fig. 3). Conversely, ACTH was more closely associated with thyroid function via new links to thyroid stimulating hormone (TSH), bound T3 and procalcitonin (PCT). Also liver functional nodes for growth factor IGF1 and C reactive protein (CRP) were no longer associated with ACTH activity in CFS. While estradiol was replaced by its precursor androstenedione (Androst), ACTH conserved strong links to aldosterone (Aldost) and its precursor progesterone (Progest) in both networks. Interestingly, the separation between ACTH and cortisol was only marginally increased in CFS ($p \sim 0.05$) using 1/MI for distance and adjusting for network size (Table 2). Cortisol was also equally proximal to the down-regulated B cell and NK cell gene sets in NF and CFS networks. This was not the case however for the remaining immune functional nodes. Monocyte, neutrophil and T cell nodes were significantly more distant from cortisol in CFS ($p \ll 0.01$). Conversely, nodes for T regulatory and up-regulated B cell gene sets were more directly associated with cortisol in CFS ($p \ll 0.01$).

The re-association of first neighbors occurring at the free T4 node is presented in Fig. 4. In CFS we observed a dramatic increase in the association of free T4 with monocyte, NK, T and B cell gene set expression and neuropeptide Y (NPY). There was also a direct association of free T4 with insulin and sex hormone-binding globulin (SHBG). Conversely, the link to estradiol was severed and testosterone (Testo) was replaced by progesterone (Progest). Similarly epinephrine was replaced by norepinephrine as a direct link between free T4 and the sympathetic nervous system in CFS.

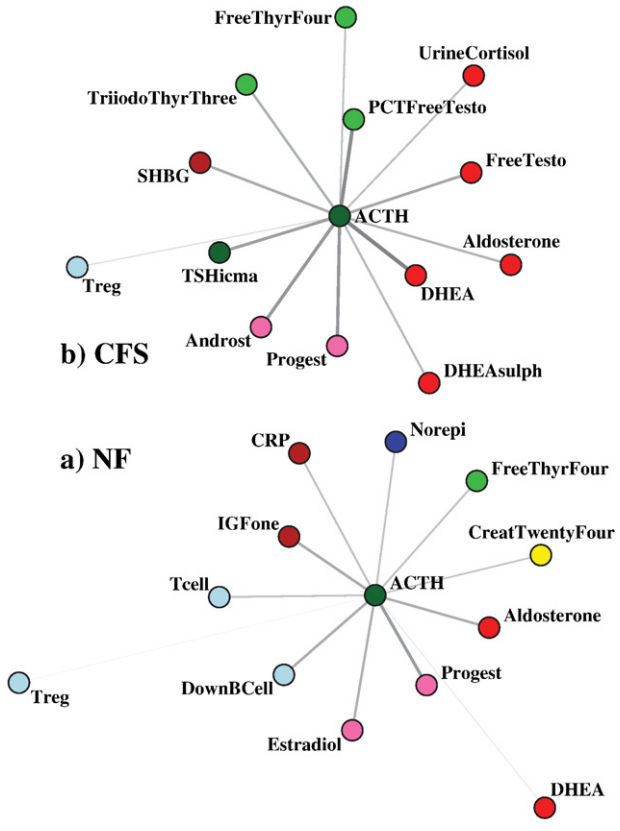

Fig. 3. ACTH dissociates from immune function in favor of thyroid in CFS. Single-node diagram showing the adrenocorticotropin hormone (ACTH) node and its first co-expressed neighbors in the networks constructed for non-fatigued (NF) subjects (a) and CFS patients (b) respectively. All links are significant at the $p \leq 0.001$. ACTH activity was decoupled from B and T cell responses in CFS and more closely associated with thyroid function.

Table 2
Statistical significance of difference in shortest path separating the cortisol node from ACTH and immune functional nodes in NF and CFS networks

Path NF	Path CFS	Delta min path[a]	Std Error[b]	*t*-ratio	*p*-value (18 *df*)
ACTH → Aldosterone →Cortisol	ACTH → FreeTesto → Cortisol	0.55	0.26	2.10	0.05
Cortisol → DownBCell	Cortisol → DownBCell	−0.06	0.21	−0.28	0.78
Cortisol → Monocytes	Cortisol → UrineCortisol → Monocytes	8.70	0.25	35.39	0.00
Cortisol → Insulin →Nkcell	Cortisol → DownBCell → Nkcell	0.42	0.29	1.42	0.17
Cortisol → Neutrophils	Cortisol → UpBCell → Neutrophils	9.13	0.31	29.66	0.00
Cortisol → UrineCortisol → Tcell	Cortisol → DownBCell → Tcell	1.59	0.32	4.95	0.00
Cortisol → DownBCell →Treg	Cortisol → Treg	−8.44	0.27	−31.76	0.00
Cortisol →Norepi →UpBCell	Cortisol → UpBCell	−9.65	0.23	−42.44	0.00

[a] Minimum path length in CFS−minimum path length in NF; both adjusted for network size.
[b] Standard error of the difference in size adjusted minimum path length.

Emergent sub-network supports chronic inflammatory response in CFS

If CFS exhibits an overactive immune response, then we expect to see a more elaborate and distributed pattern of connectivity in the CFS immune sub-network. Results in Fig. 2 show significant changes in connectivity occurred for the 7 immune functional nodes both locally and globally. Monocyte and neutrophil nodes increased their interaction, both direct and indirect, with other immune nodes and with the overall network in CFS. While the NK and down-regulated B cell (DownBCell) nodes disassociated from the overall network in CFS, they increased direct connectivity to other immune nodes. Changes in connectivity for T, T regulatory and up-regulated B cell function with the global network were marginal. However eigenvector centrality indicated that the latter two nodes re-aligned with less influential neighbors. The immune sub-networks shown in Fig. 5 were quite different with overall size increasing from 9 (NF) to 16 edges (CFS). In NF both B cell nodes were closely associated and interacted significantly with T regulatory and NK cell nodes while the T cell and neutrophil nodes formed their own sub-network. In contrast, a much more highly connected immune network emerged in CFS. The neutrophil node now maintained a strong interaction with monocyte and both B cell nodes. In what resembled a change in B cell status, the down-regulated B cell node was no longer strongly associated with its counterpart becoming instead a hub for T and NK cell activity in CFS.

Discussion

This study provided a comprehensive overview of changes in mutual information linking 37 indicators of neuroendocrine and immune function in CFS. Instead of constructing a single graph from differentially expressed nodes, we identified weighted graphs for NF and CFS separately enabling us to study characteristic changes in graph structure. Though the overall abundance of connections was conserved in both networks, they differed significantly in the distribution of highly connected nodes. Indeed the subtle re-modeling observed in CFS might well be a hallmark of many chronic disorders where homeostasis is maintained albeit with significantly altered function. CFS yielded an increase in network centrality making information flow through this network more highly dependent on a smaller number of hub nodes. In statistical physics a network increases in centrality [20] as it loses energy, a process thought to mitigate the impact of unstable feedback in living systems [21]. However in these networks the loss of a hub node is also more likely to cause catastrophic failure. Interestingly, as the neuroendocrine portion of the network re-modeled to a lower energy configuration in CFS, the immune portion morphed into a higher energy configuration.

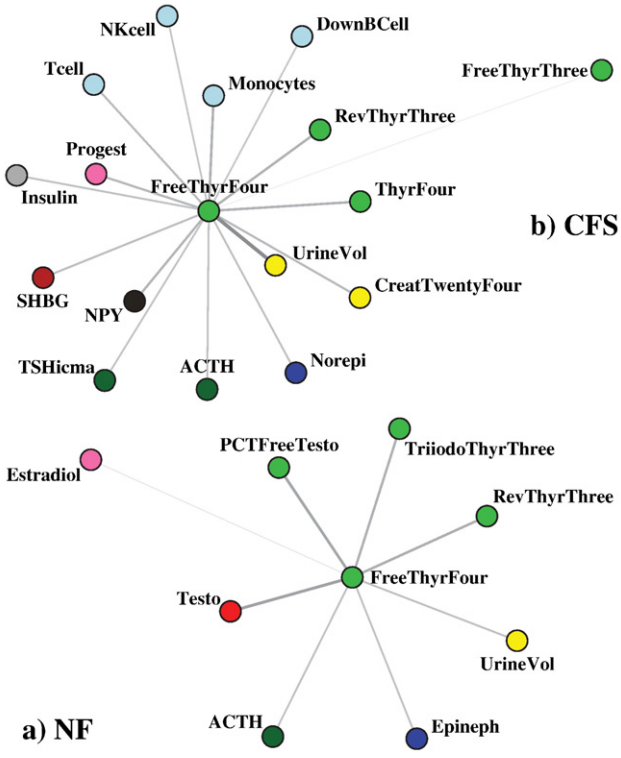

Fig. 4. Free T4 node dramatically increases interaction with immune nodes in CFS. Single-node diagram the free thyroxin T4 node and its first co-expressed neighbors in the networks constructed for non-fatigued (NF) subjects (a) and CFS subjects (b) respectively. All links are significant at the $p \leq 0.001$. A striking feature is the abundance of immune functional nodes that assume first neighbor status in the case of the CFS network.

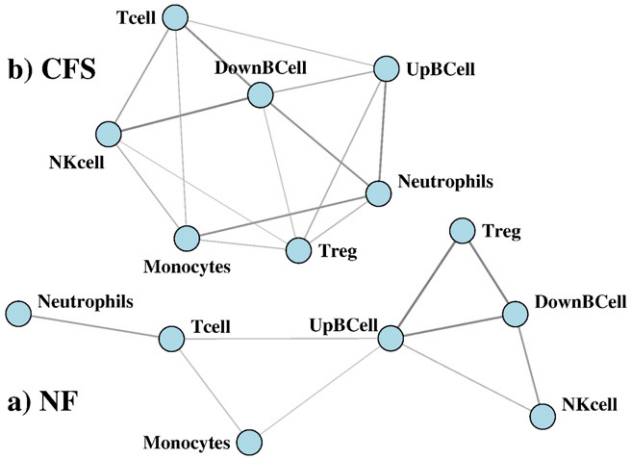

Fig. 5. Chronic inflammatory immune sub-network emerges in CFS. Mutual information sub-networks constructed for the non-fatigued (NF) (a) and CFS (b) subject groups showing co-expression patterns among the immune functional nodes only. Graph size is significantly increased in the case of the CFS immune sub-network in relation to the emergence of immune co-expression pattern absent in the NF group and characteristic of chronic inflammation.

Driving this shift in topology were significant changes in coordinated activity between the pituitary, the thyroid, the ovaries and the immune system. This was especially noticeable in terms of eigenvector centrality which doubled in CFS for nodes such as ACTH, TSH and free T4. ACTH-driven cortisol synthesis alters the cytokine profile in T cells via its effects on monocytes and other antigen-presenting cells leading to the termination of unwanted autoimmune inflammatory reactions [22]. Hypocortisolism has been observed in CFS with possible ties to ACTH unresponsiveness [23,24] and increased sensitivity to glucocorticoid [25] feedback. Interestingly the current study linked the disassociation of ACTH from immune activity in CFS to the emergence of a monocyte-neutrophil-B cell inflammatory network rooted in known immune biochemistry [26]. Despite this ongoing inflammatory response, ACTH was only marginally more distant from cortisol in CFS further supporting the notion of a loss in HPA axis control.

Inflammatory cytokines are known to inhibit thyroid function [27] and thyroid autoimmunity has been linked to diabetes and ovarian failure [28]. Recall we found a close association of free T4 with both insulin and progesterone in CFS (Fig. 4b). In fact one of the most striking results in this study involved the re-organization of network structure around the free T4 node. This node was directly linked to monocyte, NK, T and B cell nodes in CFS. Association with NPY, a monocyte mediator [29] and C reactive protein (CRP), an acute phase inflammatory protein, implicate a possible immune response directed at the thyroid. Estradiol priming is essential to thyroid function [30,31] in addition to promoting growth hormone (GH) synthesis by the pituitary and subsequently insulin-like growth factor (IGF1). IGF1 is a potent activator of cell proliferation and the resolution of inflammation. Free T4 disassociates from estradiol and testosterone in CFS acquiring instead a direct link to sex hormone-binding globulin (SHBG), a glycoprotein that suppresses bioavailability of both of the former. Reduced bioavailability of estradiol can hamper GH and IGF1 synthesis leading to deficient tissue repair consistent our observations of unresolved inflammation. Though impaired GH response has been observed in CFS [32] the current work provides novel insight into a suspected but so far unsubstantiated link to IGF1 insufficiency and inflammation.

These observations illustrate the interplay between the HPT and HPA axes. Approximately half the androstenedione, a precursor of estradiol, is produced by the adrenal glands in pre-menopausal women where it is governed by ACTH [33]. The loss of a direct link between ACTH and estradiol nodes was another indication of adrenal disturbance in CFS. As discussed previously, loss of adrenal function would have dual implications, not only releasing the inflammatory response from the control of cortisol but also impairing the cellular repair response by robbing the pituitary of estradiol stimulation in GH and IGF1 synthesis. This scenario is only exacerbated in post-menopausal women by virtue of their dependency on adrenal androstenedione and subsequent estradiol synthesis. Interestingly, there are increased rates of thyroid disease [34] and CFS [35] in women.

By conducting a comprehensive examination of the changes in neuroendocrine and immune signaling in CFS, this study provided novel evidence of a pattern of failure occurring across multiple physiological systems. Some of the changes may be linked to CFS etiology while others may reflect the body's adaptation to this chronically fatigued state. Studies of incident CFS will be needed to determine if neuroendocrine and immune network re-modeling in arises as a result of CFS or as a driver thereof.

Methods

Subject cohort

Neuroendocrine measurements and gene expression in peripheral blood mononuclear cells (PBMC) were obtained from the Wichita Clinical dataset [36] for a group of 76 female subjects screened for confounding medical or psychiatric conditions. Diagnostic classification adheres to the CFS research case definition [37] resulting in 39 CFS and 37 NF controls. Collection and processing of PBMCs including microarray hybridization are found in [36]. Details of data preprocessing, normalization, outlier detection and false discovery correction are available in [15].

Gene sets

Using data from Lyons [38], gene sets were constructed a priori from microarray profiles of CD4+ T cells, CD8+ T cells, CD19+ B cells, CD14+ monocytes and CD16+ neutrophils isolated from peripheral blood. Of 12,022 genes reported 268 were surveyed in the Wichita study. Profiles were dissected into discrete non-overlapping sets of genes preferentially induced or repressed in each lineage (>2-fold). Sets were also defined for NK and regulatory T cells resulting in 7 immune functional nodes. Node expression was computed as the mean Ln-transformed expression of each set's member genes. Additional details regarding gene set composition may be found in the supplementary data file.

Mutual information networks

Association networks were constructed using mutual information criteria (MI) implemented in the ARACNe software [19]. The mutual information MI(X;Y) shared by X and Y corresponds to the total entropy $H(X)$ and $H(Y)$ of these variables minus their joint entropy $H(X,Y)$ (Eqs. (1)–(3)). The null probability of each MI value was computed by sub-sampling with replacement. Networks for each diagnostic group were generated from a consensus of 10,000 sub-sampled networks. Network size decreased by less than 20% overall with increasing MI confidence and became asymptotically stable at $p \le 0.001$ (Supplementary Figure S1). This was used as the threshold for MI confidence in all subsequent computations. This consensus averaging across sub-sampled data sets and the fact that MI assigns equal influence to each measured value makes this approach quite robust to outliers [39,40].

$$H(X) = -\sum_{i=1}^{n} p(x_i)\log(p(x_i)) \tag{1}$$

$$H(X,Y) = -\sum_{j=1}^{n}\sum_{k=1}^{m} p(x_i,y_k)\log\left(p(x_j,y_k)\right) \tag{2}$$

$$MI(X;Y) = H(X) + H(Y) - H(X,Y) \tag{3}$$

Indirect associations were removed using data processing inequality (DPI) [41]. DPI states that if X and Z interact only through a third variable Y then Eq. (4) applies. Thus the smallest MI value can only come from indirect interaction. ARACNe removes this edge.

$$\mathrm{MI}(X,Z) \le \min\left[\mathrm{MI}(X,Y);\mathrm{MI}(Y,Z)\right] \tag{4}$$

Topological differences in networks were evaluated using a weighted graph edit distance [42] corresponding to the minimum summed "cost" associated with the removal and insertion of edges transforming one graph into the other [43,44]. Herein we make the costs of these edit operations directly proportional to the changes in edge MI. The weighted graph edit distance, d_{GED}, between two undirected networks of order N with adjacency matrices, A and B, is computed as follows where $a_{ij} = \mathrm{MI}_{ij}$ if $P(\mathrm{MI}_{ij} > 0) \ge 0.001$, else $a_{ij} = 0$ and similarly for b_{ij}:

$$d_{\mathrm{GED}} = \sum_{i=1}^{N}\sum_{j\ge i}^{N} |a_{ij} - b_{ij}| \tag{5}$$

Significance of this edit distance was estimated (i) using reference networks generated by random sub-sampling of NF subjects, (ii) from

equal-sized random networks conserving edge weight distribution [45] and (iii) through multi-graphs conserving node degree distribution [46].

Node degree centrality or direct connectivity of each node i to its immediate neighborhood N_i was computed as $\sum_{j\in N_i} a_{ij}$. Eigenvector centrality x_i was also computed for each node i as a measure of that node's connectivity to its remote neighbors. For the ith node the eigenvector centrality score x_i is proportional to the sum of x_j for all nodes connected to it such that:

$$x_i \propto \sum_{j\in N_i} x_j \Rightarrow x_i = \frac{1}{\lambda}\sum_{j\in N_i} x_j = \frac{1}{\lambda}\sum_{j=1}^{N} a_{ij}x_j \tag{6}$$

where N_i is the neighborhood of i, λ is some constant and N is the order of the network. Constraining all $a_{i,j}$ and x_i to real positive values implies, by the Perron–Frobenius theorem, that only the largest principal eigenvalue solution to Eq. (6) is accepted [47]. Finally we have also scaled the principal eigenvector X to adjust for network size as follows:

$$\hat{X} = \frac{\sqrt{2}}{||X||}X \tag{7}$$

where $\hat{X}$ is the normalized principal eigenvector and $||X||$ is the norm. This scaling is based on a maximum of $x_i = 1$ for the center node of a star network [48].

The overall degree of centralization for any network of order N and normalized principal eigenvector $\hat{X}$ is the centrality index C:

$$C_{\text{eigenvector}} = \frac{\sum_{i=1}^{N}(x_{\max} - x_i)}{\sum_{i=1}^{N}(1 - x_i)} \in [0, 1] \tag{8}$$

Graphical rendering was performed using a "spring-electrical" embedding [49] where nodes are idealized as similarly charged objects that repel each other. Edges are imagined as springs adhering to Hooke's law with spring-constants proportional to their MI weights. The network is relaxed iteratively to a minimum energy embedding.

Acknowledgments

Special thanks to Dr. Andrea Califano and the members of his laboratory at Columbia University for many helpful discussions and their assistance in deploying ARACNe. This analysis was funded by grant #52923 provided by the Faculty of Medicine and Dentistry at the University of Alberta.

Appendix A. Supplementary data

Supplementary data associated with this article can be found, in the online version, at doi:10.1016/j.ygeno.2008.08.008.

References

[1] U. Tirelli, D. Bernardi, S. Improta, A. Pinto, Immunologic abnormalities in chronic fatigue syndrome, J. Chronic Fatigue Syndrome 2 (1) (1996) 85–96.
[2] C.L. Raison, A.H. Miller, When not enough is too much: the role of insufficient glucocorticoid signaling in the pathophysiology of stress-related disorders, Am. J. Psychiatry 160 (2003) 1554–1565.
[3] S. Gupta, E. Aslakson, B.M. Gurbaxani, S.D. Vernon, Inclusion of the glucocorticoid receptor in a hypothalamic pituitary adrenal axis model reveals bistability, Theor. Biol. Med. Model 4 (2007) 8.
[4] M.J. Robertson, et al., Lymphocyte subset differences in patients with chronic fatigue syndrome, multiple sclerosis and major depression, Clin. Exp. Immunol. 141 (2) (2005) 326–332.
[5] M. Caligiuri, et al., Phenotypic and functional deficiency of natural killer cells in patients with chronic fatigue syndrome, J. Immunol. 139 (10) (1987) 3306–3313.
[6] R.B. Moss, A. Mercandetti, A. Vojdani, TNF-alpha and chronic fatigue syndrome, J. Clin. Immunol. 19 (5) (1999) 314–316.
[7] M.N. Silverman, B.D. Pearce, C.A. Biron, A. H, Review: immune modulation of the hypothalamic–pituitary–adrenal (HPA) axis during viral infection, Viral. Immunol. 18 (1) (2005) 41–78.
[8] L. Ein-Dor, O. Zuk, E. E Domany, Thousands of samples are needed to generate a robust gene list for predicting outcome in cancer, Proc. Natl. Acad. Sci. U. S. A. 103 (2006) 5923–5928.
[9] J.P. Ioannidis, Microarrays and molecular research: noise discovery? Lancet 365 (2005) 454–455.
[10] C.W. Mason, P.W. Swaan, C.P. Weiner, Identification of interactive gene networks: a novel approach in gene array profiling of myometrial events during guinea pig pregnancy, Am. J. Obs. Gyn. 194 (2006) 1513–1523.
[11] H. Savli, A. Szendr, I. Romics, B. Nagy, Gene network and canonical pathway analysis in prostate cancer: a microarray study, Exp. Mol. Med. 40 (2) (2008) 176–185.
[12] S. Efroni, C.F. Schaefer, K.H. Buetow, Identification of key processes underlying cancer phenotypes using biologic pathway analysis, PLoS ONE 2 (5) (2007) e425, doi:10.1371/journal.pone.0000425.
[13] J. Vohradsky, P. Branny, C.J. Thompson, Comparative analysis of gene expression on mRNA and protein level during development of Streptomyces cultures by using singular value decomposition, Proteomics 7 (21) (2007) 3853–3866.
[14] C.L. Barrett, N.D. Price, B.O. Palsson, Network-level analysis of metabolic regulation in the human red blood cell using random sampling and singular value decomposition, BMC Bioinformatics. 7 (2006) 132.
[15] G. Broderick, et al., Identifying illness parameters in fatiguing syndromes using classical projection methods, Pharmacogenomics 7 (3) (2006) 407–419.
[16] O. Mason, M. Verwoerd, Graph theory and networks in biology, IET Syst Biol. 1 (2) (2007) 89–119, Review.
[17] M.E. Futschik, A. Tschaut, G. Chaurasia, H. Herzel, Graph-theoretical comparison reveals structural divergence of human protein interaction networks, Genome Inform. 18 (2007) 141–151.
[18] F. Emmert-Streib, The chronic fatigue syndrome: a comparative pathway analysis, J. Comp. Biol. 14 (7) (2007) 961–972.
[19] A.A. Margolin, et al., ARACNE: an algorithm for the reconstruction of gene regulatory networks in a mammalian cellular context, BMC Bioinformatics 7 (Suppl.1) (2006) S7.
[20] I. Farkas, I. Derényi, G. Palla, T. Vicsek, Equilibrium statistical mechanics of network structures, Lect. Notes Phys. 650 (2004) 163–187.
[21] R.V. Solé, S. Valverde, Information theory of complex networks: on evolution and architectural constraints, Lect. Notes Phys. 650 (2004) 189–207.
[22] G.A. Rook, Glucocorticoids and immune function, Baillieres Best Pract. Res. Clin. Endocrinol. Metab. 13 (4) (1999) 567–581.
[23] T.C. Kamilaris, et al., Effect of altered thyroid hormone levels on hypothalamic–pituitary–adrenal function, J. Clin. Endocrinol. Metab. 65 (5) (1987) 994–999.
[24] K. Holtorf, Diagnosis and treatment of hypothalamic–pituitary–Adrenal (HPA) axis dysfunction in patients with chronic fatigue syndrome (CFS) and fibromyalgia (FM), J. Chronic Fatigue Syndrome 14 (2008) 3 (pub).
[25] F. Van Den Eede, G. Moorkens, B. Van Houdenhove, P. Cosyns, S.J. Claes, Hypothalamic–pituitary–adrenal axis function in chronic fatigue syndrome, Neuropsychobiology 55 (2) (2007) 112–120.
[26] D.L. Lefkowitz, S.S. Lefkowitz, Macrophage–neutrophil interaction: a paradigm for chronic inflammation revisited, Immunol. Cell Biol. 79 (2001) 502–506.
[27] K. Yamazaki, et al., Suppression of iodide uptake and thyroid hormone synthesis with stimulation of the type I interferon system by double-stranded ribonucleic acid in cultured human thyroid follicles, Endocrinology 148 (7) (2007) 3226–3235.
[28] R. Goswami, et al., Prevalence of thyroid autoimmunity in sporadic idiopathic hypoparathyroidism in comparison to type 1 diabetes and premature ovarian failure, J. Clin. Endocrinol. Metab. 91 (11) (2006) 4256–4259.
[29] J. Wheway, et al. A fundamental bimodal role for neuropeptide Y1 receptor in the immune system, J. Exp. Med. 202 (11) (2005) 1527–1538.
[30] G.I. Khodorovskii, Sex differences in response of the thyroid gland and its sensitivity to thyrotropic hormone after administration of estradiol, testosterone, and progesterone, Bull. Exp. Biol. Med. 82 (3) (1976) 1391–1393.
[31] S.K. Banua, P. Govindarajulua, M.M. Aruldhasa, Testosterone and estradiol differentially regulate TSH-induced thyrocyte proliferation in immature and adult rats, Steroids 67 (7) (2002) 573–579.
[32] G. Moorkens, J. Berwaerts, H. Wynants, R. Abs, Characterization of pituitary function with emphasis on GH secretion in the chronic fatigue syndrome, Clin. Endocrinol. (Oxf) 53 (1) (2000) 99–106.
[33] J.L. Shifren, I. Schiff, The aging ovary, J. Women's Health and Gender-based Med. 9 (Suppl. 1) (2000) S3–S7.
[34] Y. Aoki, et al., Serum TSH and Total T4 in the United States population and their association with participant characteristics: National Health and Nutrition Examination Survey (NHANES 1999–2002), Thyroid 17 (12) (2007) 1211–1223.
[35] S. Hempel, D. Chambers, A.M. Bagnall, C. Forbes, Risk factors for chronic fatigue syndrome/myalgic encephalomyelitis: a systematic scoping review of multiple predictor studies, Psychol Med. (2007) 1–12 [Epub ahead of print]
[36] S.D. Vernon, W.C. Reeves, The challenge of integrating disparate high-content data: epidemiological, clinical and laboratory data collected during an in-hospital study of chronic fatigue syndrome, Pharmacogenomics 7 (3) (2006) 345–354.
[37] W.C. Reeves, et al., Chronic fatigue syndrome — a clinically empirical approach to its definition and study, BMC Medicine 3 (2005) 19.
[38] P.A. Lyons, et al., Microarray analysis of human leucocyte subsets: the advantages of positive selection and rapid purification, BMC Genomics 8 (2007) 64.
[39] R.C. Craddock, et al., Exploration of statistical dependence between illness parameters using the entropy correlation coefficient, Pharmacogenomics 7 (3) (2006) 421–428.

[40] A.J. Butte, I.S. Kohane, Mutual information relevance networks: functional genomic clustering using pairwise entropy measurements, Pac. Symp. Biocomput. (2000) 418–429.
[41] T.M. Cover, J.A. Thomas, Elements of Information Theory, John Wiley and Sons, New York, 1991.
[42] H. Bunke, Graph matching: theoretical foundations, algorithms, and applications, Proc. Vision Interface 2000, Montreal (2000) 82–88.
[43] P. Dickinson, H. Bunke, A. Dadej, M. Kraetzl, Matching Graphs with Unique Node Labels, Pattern Analysis and Applications 7 (2004) 243–254.
[44] G. Harper, G.S. Bravi, S.D. Pickett, J. Hussain, D.V. Green, The reduced graph descriptor in virtual screening and data-driven clustering of high-throughput screening data, J. Chem. Inf. Comput. Sci. 44 (6) (2004) 2145–2156.
[45] R. Milo, N. Kashtan, S. Itzkowitz, M.E.J. Newman, U. Alon, On the uniform generation of random graphs with prescribed degree sequences, arXiv:cond-mat/0312028v2 [cond-mat.stat-mech] (2004).
[46] M.E.J. Newman, Analysis of weighted graphs, Phys. Rev. E 70 (5) (2004) 56131–1–56131–9.
[47] J.M. Kleinberg, Authoritative Sources in a Hyperlinked Environment, J. Assoc. Comp. Mach. 46 (5) (1999) 604–632.
[48] B. Ruhnau, Eigenvector-centrality — a Node Centrality? Social Networks 22 (2000) 357–365.
[49] S. Pemmaraju, S. Skiena, Computational Discrete Mathematics: Combinatorics and Graph Theory with Mathematica®, Cambridge University Press, Cambridge and New York, 2003, pp. 220–223.